AGU PUBLICATIONS

JGR

Journal of Geophysical Research: Biogeosciences

RESEARCH ARTICLE
10.1002/2016JG003386

Key Points:
- The two partitioning approaches, trenching and ^{14}C, quantified autotrophic, and heterotrophic sources of the soil CO_2 flux differently
- Incorporating these partitioning data constraints in a model-data fusion framework greatly reduces model uncertainties of soil C fluxes
- The impact of these constraints on modeled soil C pool sizes is small in future climate and CO_2 scenarios without additional constraints

Supporting Information:
- Supporting Information S1

Correspondence to:
M. S. Carbone,
mariah.carbone@unh.edu

Citation:
Carbone, M. S., A. D. Richardson, M. Chen, E. A. Davidson, H. Hughes, K. E. Savage, and D. Y. Hollinger (2016), Constrained partitioning of autotrophic and heterotrophic respiration reduces model uncertainties of forest ecosystem carbon fluxes but not stocks, *J. Geophys. Res. Biogeosci.*, *121*, 2476–2492, doi:10.1002/2016JG003386.

Received 18 FEB 2016
Accepted 11 AUG 2016
Accepted article online 15 AUG 2016
Published online 22 SEP 2016

Constrained partitioning of autotrophic and heterotrophic respiration reduces model uncertainties of forest ecosystem carbon fluxes but not stocks

Mariah S. Carbone[1], Andrew D. Richardson[2], Min Chen[2], Eric A. Davidson[3], Holly Hughes[4], Kathleen E. Savage[4], and David Y. Hollinger[5]

[1]Earth Systems Research Center, University of New Hampshire, Durham, New Hampshire, USA, [2]Department of Organismic and Evolutionary Biology, Harvard University, Cambridge, Massachusetts, USA, [3]Appalachian Laboratory, University of Maryland Center for Environmental Science, Frostburg, Maryland, USA, [4]Woods Hole Research Center, Falmouth, Massachusetts, USA, [5]USDA Forest Service, Northern Research Station, Durham, New Hampshire, USA

Abstract We partitioned the soil carbon dioxide flux (R_s) into its respective autotrophic and heterotrophic components in a mature temperate-boreal forest (Howland Forest in Maine, USA). We combined automated chamber measurements of R_s with two different partitioning methods: (1) a classic root trenching experiment and (2) a radiocarbon (^{14}C) mass balance approach. With a model-data fusion approach, we used these data to constrain a parsimonious ecosystem model (FöBAAR), and we investigated differences in modeled C fluxes and pools under both current and future climate scenarios. The trenching experiment indicated that heterotrophic respiration accounted for 53 ± 11% of total R_s. In comparison, using the ^{14}C method, the heterotrophic contribution was 42 ± 9%. For both current and future model runs, incorporating the partitioning data as constraints substantially reduced the uncertainties of autotrophic and heterotrophic respiration fluxes. Moreover, with best fit model parameters, the two partitioning methods yielded fundamentally different estimates of the relative contributions of autotrophic and heterotrophic respiration to total R_s, especially at the annual time scale. Surprisingly, however, modeled soil C and biomass C pool size trajectories did not differ significantly between model runs based on the different methods. Instead, model differences in partitioning were compensated for by changes in C allocation, resulting in similar, but still highly uncertain, soil C pool trajectories. Our findings show that incorporating constraints on the partitioning of R_s can reduce model uncertainties of fluxes but not pools, and the results are sensitive to the partitioning method used.

1. Introduction

The soil carbon dioxide flux (R_s) is one of the largest fluxes in the terrestrial carbon (C) cycle, and in most ecosystems it is second in magnitude only to photosynthesis [*Raich and Schlesinger*, 1992]. R_s is primarily the combination of two sources: autotrophic respiration (R_a), which is the CO_2 produced from plant root metabolism and associated microbial respiration, and heterotrophic respiration (R_h), which is CO_2 from free-living microbial decomposition of soil organic matter (SOM).

R_a and R_h are thus large components of the terrestrial C cycle, but they are also among the most poorly constrained in ecosystem C budgets [*Schulze et al.,* 2010] principally because they are hard to separate and quantify with field measurements. Methods to partition these fluxes in intact ecosystems include root exclusion (e.g., girdling and trenching) and isotopic approaches (e.g., natural abundance and labeling studies with ^{13}C and ^{14}C). Each partitioning approach has advantages and disadvantages that have been thoroughly reviewed [*Hanson et al.*, 2000; *Kuzyakov*, 2006; *Subke et al.,* 2006]. The disadvantages, which often limit implementation, include substantial labor as well as financial expense. Additionally, these methods can be very destructive to both the vegetation and the soil. And, while R_a and R_h can be estimated using simplified relationships based on temperature, the associated uncertainties are large [*Trumbore*, 2006]. Thus, in many ecosystem-level studies, R_a and R_h remain unquantified—or, at best, poorly quantified—fluxes.

Quantifying the contributions of autotrophic and heterotrophic sources to R_s is important for improving models that predict how environmental and biological factors influence ecosystem C cycling and storage. For example, both R_a and R_h are sensitive to environmental factors such as temperature and moisture; however, their responses to these factors may be different [*Boone et al.,* 1998; *Pregitzer et al.,* 2000; *Heinemeyer et al.,* 2007; *Gu et al.,* 2008]. R_a may also be influenced by plant phenology, including seasonal

changes in root biomass and root exudation, as well as overall above and belowground plant activity [*Davidson and Holbrook*, 2009; *Kuzyakov and Gavrichkova*, 2010; *Savage et al.,* 2013]. R_h, on the other hand, may be affected by both the quality and quantity of SOM (e.g., fresh litter inputs) as well as soil mineral properties [*Moyano et al.,* 2012].

The lack of mechanistic information on how R_a and R_h (and their uncertainties) vary seasonally across different ecosystems limits our ability to test and improve how belowground processes are represented and parameterized in ecosystem models. For example, *Keenan et al.* [2011] showed that without direct observational constraints for R_a and R_h (but using other data constraints such as R_s, net ecosystem exchange of CO_2, and biometric measurements), a model-data fusion approach could not be used to partition R_s, because the estimated uncertainties on these two sources were so large. Moreover, model estimates of R_a and R_h were strongly negatively correlated with each other (which is biologically implausible), because the same R_s could be achieved with an increase in R_a (or R_h) and a decrease in R_h (or R_a). Inadequate characterization of these uncertainties leads to overconfidence in model forecasts of ecosystem C storage in response to future environmental change. However, integrating isotopic data with models has been shown to be a powerful approach for estimating C pool sizes and turnover times and for separating respiration sources [*Zobitz et al.,* 2008; *Ahrens et al.,* 2014; *Ogle and Pendall*, 2015]. Because R_h is the major loss pathway of terrestrial C stocks back to the atmosphere, this should help to improve model-based estimates of the future trajectories of terrestrial C sequestration.

In this study, our objective was to assess how data on partitioning of R_s influences ecosystem C cycle simulations for both present-day and future environmental scenarios. To do this, we partitioned R_s, measured at high temporal frequency using an automated chamber system, into its respective autotrophic and heterotrophic components, with (1) a classic root trenching experiment and (2) an isotopic mass balance approach, using the radiocarbon (^{14}C) bomb spike. We then used R_s and the separate partitioning information as observational constraints for simulating C fluxes and stocks using a model-data fusion approach. For this, we used long-term measurements of ecosystem C pools and fluxes, from the Howland Forest AmeriFlux site in Maine, USA, and the parsimonious ecosystem model, FöBAAR [*Keenan et al.,* 2012].

Our analysis focuses on the following questions: (1) Do the two different partitioning approaches give comparable results?; and (2) How does including R_s and partitioning data as constraints impact model simulations of C fluxes and stocks? Our overarching hypothesis is that uncertainty in rates of SOM accretion is largely driven by uncertainty about whether R_s is coming from autotrophic or heterotrophic sources. Specifically, we hypothesize that better constraints on the partitioning of R_s reduces uncertainties on soil C stocks because the partitioning allows us to narrow uncertainties on R_h and hence C losses from the soil pool.

2. Material and Methods

2.1. Site and Experimental Design

The Howland Forest is a temperate-boreal transitional forest located in central Maine, USA, about 60 km north of Bangor. It is an AmeriFlux site, where tower-based eddy covariance measurements of surface-atmosphere exchanges of CO_2, water, and energy have been made since 1996. Mean annual temperature at the site is 5.4°C, and mean annual precipitation is 1050 mm, spread evenly throughout the year. The vegetation is dominated by mature red spruce (*Picea rubens* Sarg.) and eastern hemlock (*Tsuga canadensis* (L.) Carr.) trees dating from the middle to late 1800s. The soils are glacial tills, acid in reaction, with low fertility and high organic composition. They are classified as Orthic Humo-Ferric Podzols (Typic and Aquic Haplorthods) [*Fernandez et al.,* 1993].

Automated measurements of R_s have been conducted annually since 2004 within the footprint of the tower on upland soil [see *Savage et al.*, 2008, 2009]. To partition R_s into R_a and R_h, we used both root trenching and ^{14}C mass balance approaches. Both methods operationally define R_a as all the CO_2 derived from root metabolism, root symbionts, and microbes decomposing fresh root exudates, typically called rhizosphere respiration. R_h is defined as the CO_2 produced from microbial and faunal decomposition of SOM.

2.2. Automated Measurements of R_s

The automated R_s measurement system is fully described in *Savage and Davidson* [2003]. Briefly, the system consisted of six dark chambers. The chamber tops were constructed of white PVC (35.5 cm diameter and

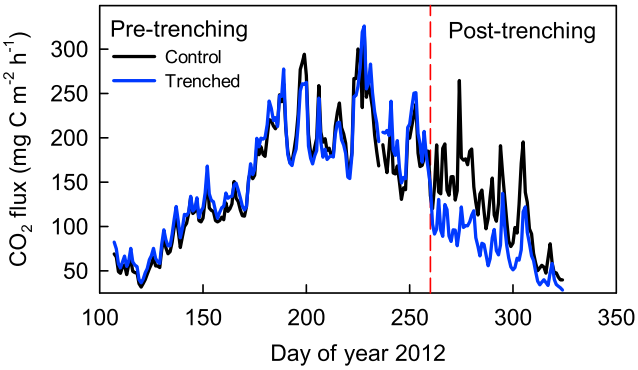

Figure 1. Mean daily CO_2 flux (mg C m^{-2} h^{-1}) from Howland Forest May to November 2012 for control chambers (black) and trenched chambers (blue). Trenching occurred on DOY 260 and is marked by a red dashed line.

15 cm tall) with gas inlet and outlet ports on top. Chamber collars were 6.5 cm tall PVC inserted 2 cm in to the soil profile. To make a measurement, the chamber tops were automatically lowered with a pneumatic piston and sealed to the collars with a neoprene gasket. All chambers were located within a 50 m radius of a central manifold system that controlled the raising and lowering of the chamber tops, gas flow to and from the chambers, and recorded temperature (type *T* thermocouple) and moisture (CS616, Campbell Scientific, Logan, UT, USA) at 10 cm depth in the soil of each chamber collar on a datalogger (Campbell Scientific CR10X). During a measurement, gas from each chamber was routed through the central box via solenoid valve-controlled manifolds to a Picarro G2121-i Isotopic Carbon-Analyzer (Picarro Inc., Santa Clara, CA, USA) in a nearby climate-controlled instrument shed, which measured the concentration of CO_2 (ppm) and $\delta^{13}CO_2$ (‰) approximately once per second. Air was recirculated through the chamber, and the flux was calculated based on the slope of the increase in CO_2 over time. Each chamber was measured every 90–120 min from early May to early November in 2013, encompassing the snow-free portion of the year. All fluxes were calculated and quality controlled using established methods described in *Savage et al.* [2008]. Missing data were filled by linear interpolation. R_s is reported here (mg C m^{-2} h^{-1}) as the mean of the three chambers for each treatment (trenched and control, see below). Cumulative R_s (g C m^{-2}) is the aggregated sum of the hourly measurements.

2.3. Root Trenching Experiment

We removed the autotrophic component of R_s in three (or half) of the automated chambers by excavating trenches around these chambers in September 2012. The specific three chambers were selected using the 2012 growing season data, ensuring that the mean fluxes from each treatment, i.e., trenched chambers and those in undisturbed soil (control chambers), were approximately equivalent prior to trenching (Figure 1). Each of the three trenched areas was approximately 3 m × 3 m. Soil was excavated to 0.6 m depth with a small backhoe (deep enough to exclude most, if not all, of the fine and coarse roots, as the overwhelming majority of root biomass is found in the upper 20 cm of the soil at this site). The trenches were then lined with 6 mil polyethylene plastic to prevent new roots from growing into the area. Soil horizons were carefully placed back in the trenches to minimize disturbance to the ecosystem. We define the flux measured by the control chambers as R_s, the flux measured by the trenched chambers as R_h, and the difference between the two fluxes (control minus trenched) as R_a. Uncertainties are reported as the standard deviation across the three chambers for R_s and R_h. These errors were added in quadrature for R_a.

2.4. Isotope Measurements for the Mass Balance Approach

We used ^{14}C measurements of respired CO_2 and a two end-member isotope mixing model to estimate the autotrophic and heterotrophic contribution to R_s from the undisturbed soil chambers (control chambers) [*Gaudinski et al.*, 2000]. This separation is possible because of the near-doubling of ^{14}C in the atmosphere by aboveground nuclear weapons testing in the 1950s and 1960s, called the "bomb spike." Since then, atmospheric ^{14}C has declined due to exchange with ocean and land reservoirs and thus provides an annual tracer that can be used to age organic matter assimilated since the bomb spike occurred. R_a and R_h often have very different ^{14}C signatures because R_a usually reflects recently assimilated C (younger, less bomb ^{14}C), whereas R_h usually reflects a range of different ages, but on average decadal cycling C (older, more bomb ^{14}C) [*Trumbore*, 2006].

Collections of the ^{14}C in respiration from all chambers were taken 4 times over the growing season of 2013, in mid-June, July, August, and September. Control chamber collections represent the $^{14}CO_2$ in R_s, while the trenched chamber collections represent intact measurements of the $^{14}CO_2$ of R_h (one end-member). To collect

the $^{14}CO_2$, the chambers tops were closed, and the chambers operated in a flow-through mode with CO_2-free air added to control the concentration of CO_2 to approximately ambient levels so that the change in concentration in the chamber space did not alter the gradient of CO_2 from the soil surface to the atmosphere. Once stabilized, the $\delta^{13}CO_2$ was recorded on a Picarro G1101-i Isotopic Carbon-Analyzer (Picarro Inc.), and air from the chamber was then directly routed into a vacuum line where CO_2 was cryogenically trapped and purified.

During three of the four monthly sampling periods, incubations of excised roots were conducted to determine the R_a end-member, following *Carbone et al.* [2008]. Fine roots (<2 mm diameter) from five hemlock and five spruce trees were collected separately. Roots from each species were rinsed with deionized water and placed in a separate airtight 1 L Mason jars with gas inlets and outlets on the lids. The jars were flushed with CO_2-free air and put in a cool room to maintain temperatures close to field conditions. The CO_2 was allowed to accumulate to at least 2000 ppm (~2 h), before the $\delta^{13}CO_2$ was recorded, and the remaining CO_2 in the air cryogenically purified by attaching the jars to the vacuum line.

SOM was also incubated once in mid-July as an additional measure of the R_h end-member, following *Schuur and Trumbore* [2006]. Intact litter/soil blocks were excavated with a shovel to the depth of the organic layer (6–17 cm) from the footprint of each of the six chambers (but not inside the collar). Larger roots (>0.5 mm) were gently removed, and soil was placed in separate 1 l Mason jars, flushed with CO_2-free air, and left to sit at ambient temperature. The CO_2 concentration in each jar was measured every 2 days to monitor the rate of CO_2 production and to ensure CO_2 concentrations did not exceed soil gas CO_2 values observed in the field. After a 7 day waiting period (based on prior work, enough time for very fine roots to cease respiration, and disturbance effects to be minimal) each jar was flushed with CO_2-free air and left to accumulate CO_2 for 1–2 days. Aliquots from the jars were then passed through the Picarro to measure the $\delta^{13}CO_2$, and the remaining air was directly routed into a vacuum line where CO_2 was cryogenically purified. While this incubation measurement captures the ^{14}C signature of the microbially decomposed fast cycling C, including root exudates and new litter inputs, some of the fastest cycling C may be underestimated because it is decomposed during the waiting period.

Finally, we also collected samples of ambient air to quantify the site-specific background atmospheric $^{14}CO_2$ and also as a measure of the signature of new photosynthetic products. During the July and August samplings, an atmospheric air sample was taken on the top of the eddy covariance tower at 27 m height with a preevacuated 6 L canister that filled slowly over 4 h. Canisters were subsequently evacuated on a vacuum line, and the CO_2 was cryogenically purified. We also grew annual chia (*Salvia hispanica*) plants on the top of the tower over the course of the summer. The ^{14}C in annual plants reflects that of the atmosphere; therefore, the plant biomass is a good measure of the time-integrated atmospheric $^{14}CO_2$. We harvested old plants and started growing new plants, approximately every 2 weeks from the beginning of July to the end of September. Plants were oven dried and ground with a mortar and pestle.

2.5. ^{14}C Analyses

Glass vials of the purified CO_2, as well as the dried annual plant samples, were sent to U.S. Department of Agriculture (USDA) Forest Service Northern Research Station Laboratory in Houghton, MI, where they were converted to graphite [*Vogel et al.,* 1987]. The ^{14}C content of the graphite was measured using accelerator mass spectrometry (AMS) at the Center for Accelerator Mass Spectrometry at Lawrence Livermore National Laboratory [*Davis et al.,* 1990]. The data ($\Delta^{14}C$) are reported in per mil (‰), the deviation of the ratio of $^{14}C/^{12}C$ in a sample divided by that of a standard of fixed isotopic composition (0.95 times the $^{14}C/^{12}C$ of oxalic acid I standard, decay corrected to 1950). The measurements have been corrected for the effects of mass-dependent isotope fractionation by normalizing to a common $\delta^{13}C$ value (−25‰) and assuming ^{14}C fractionation is twice that of ^{13}C [*Stuiver and Polach*, 1977], using the Picarro $\delta^{13}CO_2$ measurements described previously.

2.6. Mixing Model for Partitioning

The single-isotope, two-source mixing model, and error propagation methods from *Phillips and Gregg* [2001] were applied to partition R_s with the following equation:

$$\Delta^{14}C_T = \Delta^{14}C_a \times F_a + \Delta^{14}C_h \times (1 - F_a) \quad (1)$$

where $\Delta^{14}C_T$ is the mean ^{14}C signature from the three control chambers for each of the sampling time points. The autotrophic end-member is $\Delta^{14}C_a$, determined by the mean ^{14}C signature of the root incubations. The

heterotrophic end-member is $\Delta^{14}C_h$, determined by the mean ^{14}C signature of the SOM incubations and the trenched chamber respiration. The fraction of respiration from autotrophic sources is F_a, and the fraction of respiration from heterotrophic sources is thus 1-F_a.

We tested for significance of differences between the means of the $\Delta^{14}C_a$ and $\Delta^{14}C_h$ end-members using a Student's *t* test and between means across the four sampling time points using repeated measures analysis of variance.

To estimate R_a and R_h fluxes, the partitioning fractions for each time point were multiplied by the mean daily flux of the control chambers for 5 days surrounding the ^{14}C sampling time period. Uncertainties were combined in quadrature and include both the spatial and temporal uncertainty associated with the chamber flux measurements, as well as the uncertainty in the ^{14}C measurements, as propagated through the mixing model.

2.7. Modeling

We used model-data fusion methods to investigate the ecosystem-scale impacts of different assumptions about the partitioning of R_s into R_a and R_h. To do this, we applied a multiple-constraints approach and an optimization framework based on Monte Carlo methods [*Richardson et al.,* 2010] to estimate the model parameters and the initial values of ecosystem state variables for the FöBAAR model [*Keenan et al.,* 2012]. Following *Raupach et al.* [2005], our approach also places special emphasis on integration of information on data uncertainties, which are fully propagated through the analytical framework. We used the methods described by *Richardson et al.* [2010] to characterize data uncertainties.

FöBAAR (Forest Biomass, Assimilation, Allocation, and Respiration) is an ecosystem C cycle model that operates on a half-hourly timescale. It tries to balance parsimony with more detailed process representation. Fully described in *Keenan et al.* [2012], the model uses two canopy layers (Sun and shade) to calculate photosynthesis following a Farquhar-type approach. Autotrophic respiration is calculated for three biomass pools (foliage, wood, and roots), while heterotrophic respiration and decomposition are calculated for four soil C pools (litter, as well as fast, slow, and passive SOM). The model is driven by air temperature, soil temperature, photosynthetically active radiation, vapor pressure deficit, precipitation, and atmospheric CO_2.

In FöBAAR, fluxes from the soil C pools, including both R_h and decomposition fluxes, are calculated separately at each time step for the litter pool and each of the three (fast, slow and passive) SOM pools. The respiration fluxes return CO_2 to the atmosphere, and the decomposition fluxes pass C to the next more recalcitrant soil C pool (e.g., litter → fast → slow → passive). Respiration fluxes are computed as $F = Pt$, where F is the flux, P is the pool size, and t is a turnover rate, which is the product of a base rate and a Q_{10}-style temperature sensitivity. Separate base rate parameters are used for each pool. Two temperature sensitivity parameters are used, one that applies to the litter pool and one that applies to all three SOM pools. Decomposition fluxes are computed as a fixed proportion of the respiration flux from each pool, but the proportion varies among pools. Respiration and decomposition from the litter pool are driven by air temperature, whereas for the SOM pools they are driven by soil temperature. Aboveground and belowground autotrophic respiration fluxes are calculated as the product of the pool size (here, foliage biomass, and above and belowground woody biomass) multiplied by a turnover rate, which is again the product of a base rate and a Q_{10}-style temperature sensitivity. The base rate and temperature sensitivity parameters are optimized separately for each autotrophic respiratory flux. Aboveground autotrophic respiration is driven by air temperature, whereas belowground autotrophic respiration is driven by soil temperature.

As observational constraints, we used R_s measured by automated chambers and partitioning estimates described here, as well as ecosystem-scale CO_2 and H_2O fluxes measured, since 1996, by eddy covariance at the "main" Howland AmeriFlux tower [*Hollinger et al.,* 2004], and biometric measurements of woody biomass and biomass increment, leaf area index, and litterfall [*Richardson et al.,* 2010]. We partitioned the total soil C pool (data from *Fernandez et al.* [1993]) using SOM proportions and ^{14}C-based estimates of turnover times from S. Trumbore (personal communication, 2011) based on methods described in *Gaudinski et al.* [2000]. Initial (i.e., the start of the simulation period: 1996) SOM pool sizes were 1100, 5500, and 4400 g C m^{-2} for fast, slow, and passive soil C pools, respectively. The initial size of the litter pool was treated as an optimized parameter. The turnover times, which were optimized, were constrained to prior ranges of

1–10 years, 1–2 years, 30–100 years, and 500–2000 years for the litter, fast, slow, and passive SOM pools, respectively.

We conducted the model optimization using 18 years of data from 1996 to 2013 ("current climate" runs), and then we ran the optimized model forward to 2100 ("future climate" runs) for Howland using downscaled data derived from Coupled Model Intercomparison Project phase 5 runs of the National Center for Atmospheric Research Community Climate System Model under the Representative Concentration Pathways RCP 8.5 scenario [*Brekke et al.,* 2013]. Under this scenario, Earth's mean annual temperature is predicted to increase by more than 4°C.

Following *Press et al.* [1993], we used a chi-square test to determine which parameter sets were consistent with the observational data at 90% confidence. The range of model predictions from these posterior parameter sets additionally allows us to specify uncertainties on model states and fluxes [*Richardson et al.,* 2010]. We have benchmarked our approach in several model-data fusion intercomparison experiments [*Trudinger et al.,* 2007; *Fox et al.,* 2009].

We compared four different parameterizations of FöBAAR, which differed only in the R_s and partitioning data used as constraints. All runs were also constrained by tower fluxes, litterfall, woody biomass increment, and leaf area index constraints. The four model cases were (1) R_s-null run: No R_s data used as constraints, (2) R_s-autochamber run: automated chamber measurements of R_s used as constraints, (3) R_s-isotope run: automated chamber measurements of R_s plus ^{14}C-based partitioning estimates used as constraints, and (4) R_s-trenching run: automated chamber measurements of R_s plus partitioning estimates from the trenched plots used as constraints. We recognize the importance of the tower-based flux data by giving the uncertainty-weighted RMSE a multiplier of 5 in the cost function, compared to a multiplier of 1 for all other data streams.

3. Results

3.1. Environmental Conditions and CO_2 Fluxes

R_s followed a typical [e.g., *Davidson et al.*, 2006] seasonal pattern for Howland Forest. With the exception of large fluxes following two large rain events near day of year (DOY) 250, the maximum fluxes for all chambers were reached between DOY 182 and 243 when soil and air temperatures were greatest (Figure 2).

The 2013 growing season (May–September) average temperature was 16.7°C, which was close to the 1996–2013 average of 16.6 ± 0.8°C. However, with 575 mm precipitation, the 2013 growing season was somewhat wetter than the 18 year average (515 mm). Soil temperature was the same between the control and trenched chambers, with a mean value of 12.8°C over the measurement period. Surprisingly, the surface soil moisture was slightly lower in the trenched chambers with a mean of 0.14 m^3 H_2O m^{-3}soil compared to 0.19 m^3 H_2O m^{-3} in the control chambers; however, this difference existed prior to the trenching and continued for the entire measurement period. Trenched and control minus trenched chamber fluxes were similar in magnitude and had comparable seasonal patterns. Of the four ^{14}C sampling time periods, DOY 167 was the coolest and wettest, while both DOY 200 and 227 were warmer and drier, and DOY 267 was again cooler and wetter (Table 1). Integrated over the growing season, the flux from the trenched chambers (R_h) was equal to 53 ± 11% (±1 SE) of the control chamber flux (R_s).

3.2. ^{14}C of Respiration

The Δ^{14}C signatures of the atmosphere, root and SOM incubations, and R_s flux, as described below, are summarized in Figure 3. The mean Δ^{14}C signature of the atmosphere sampled by the annual plants and canisters was 18.0 ± 1.0‰ (±1 SE, n = 7), which is slightly below the Northern Hemispheric record value at Point Barrow, AK, for that same time period (23.4 ± 1.0‰, ±1 SE, n = 10, X. Xu, personal communication, 2014).

The mean Δ^{14}C signature of root respiration ranged between 31.8 and 34.7‰ over the growing season with no significant differences among sampling periods. The mean Δ^{14}C signature of root respiration across all sampling periods, 33.3 ± 1.9‰ (±1 SE, n = 6 incubations), was thus used as the R_a end-member. This value is elevated above atmospheric measurements and thus suggests some contribution of older stored nonstructural carbohydrates fueling root respiration in these trees [*Carbone et al.,* 2011].

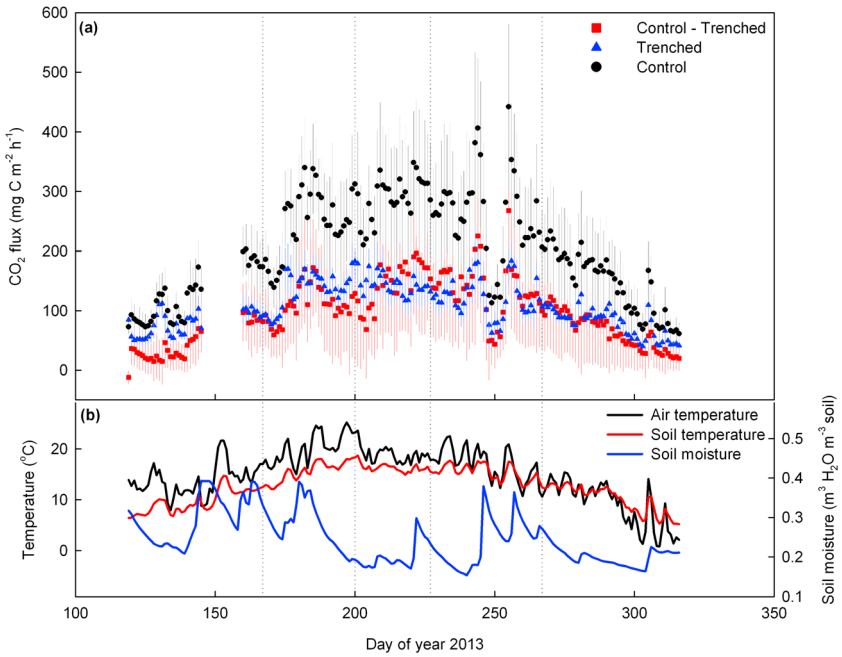

Figure 2. (a) Mean daily R_s flux (mg C m^{-2} h^{-1}) from Howland Forest May to November 2013 for control chambers (black circles), trenched chambers (blue triangles), and control minus trenched chambers (red squares). Error bars represent ±1 SD across the ($n = 3$) chambers. (b) Mean daily air temperature (black), soil temperature at 10 cm depth (red), and soil moisture at 20 cm depth (blue). In both panels, dotted vertical lines represent the days where ^{14}C was sampled.

The $\Delta^{14}C$ signatures of the trenched chamber respiration, which varied significantly among sampling periods ($p < 0.05$), were lowest on DOY 167 and 267 and highest on DOY 200 and 227. Overall, the mean $\Delta^{14}C$ signature of the trenched chamber respiration was 69.9 ± 5.5‰ (±1 SE, $n = 4$ sampling dates). This value is similar to the $\Delta^{14}C$ signature of the SOM incubations from DOY 200 (80.3 ± 5.4‰, mean ±1 SE, $n = 6$ incubations), as well as the trenched chamber respiration that was collected at the same time (75.6 ± 4.9‰, mean ± 1 SE, $n = 3$ chambers). We present our main modeling results using the R_h end-member calculated as the mean $\Delta^{14}C$ signature of all trenched chamber respiration and SOM incubations (73.4 ± 2.9‰, mean ± 1 SE, $n = 18$ samples), because we believe that it is more spatially and temporally representative. However, we also conducted our modeling analyses using the seasonally varying trenched chamber respiration as the R_h end-member. The differences between these two approaches are discussed below. The $\Delta^{14}C$ signatures of the control (untrenched) chamber respiration were not significantly different across the sampling time points ($p = 0.3$).

3.3. Source Partitioning

The $\Delta^{14}C$ signatures of the R_a and R_h end-members were significantly ($p < 0.001$) different from each other. Control chamber respiration signatures fell between these two end-members, which allowed for robust partitioning results. The temporal pattern of partitioning (Figure 4) was driven by relatively small, nonsignificant changes in the ^{14}C signature of the control plots (Figure 3). The R_a fraction (fraction of total respiration from autotrophic sources) ranged from 0.44 ± 0.11 to 0.65 ± 0.08, with the largest contribution on DOY 227 (±1 SE, Figure 4). The R_h fraction (fraction of total respiration from heterotrophic sources) ranged between 0.35 ± 0.08

Table 1. Mean Daily Air Temperature, Soil Temperature at 10 cm Depth, and Soil Moisture at 10 cm Depth in the Control and Trenched Chambers at Howland Forest During the Time Periods When ^{14}C Was Sampled

Sampling Month	Day of Year	Air Temperature (°C)	Soil Temperature (°C)		Soil Moisture (m^3 H_2O m^{-3} Soil)	
			Control	Trenched	Control	Trenched
June	167	16.8	12.5	12.3	0.21	0.16
July	200	22.9	18.1	18.2	0.16	0.14
August	227	18.2	15.7	15.6	0.18	0.14
September	267	12.8	13.2	13.1	0.19	0.15
Average	-	15.0	12.8	12.7	0.19	0.14

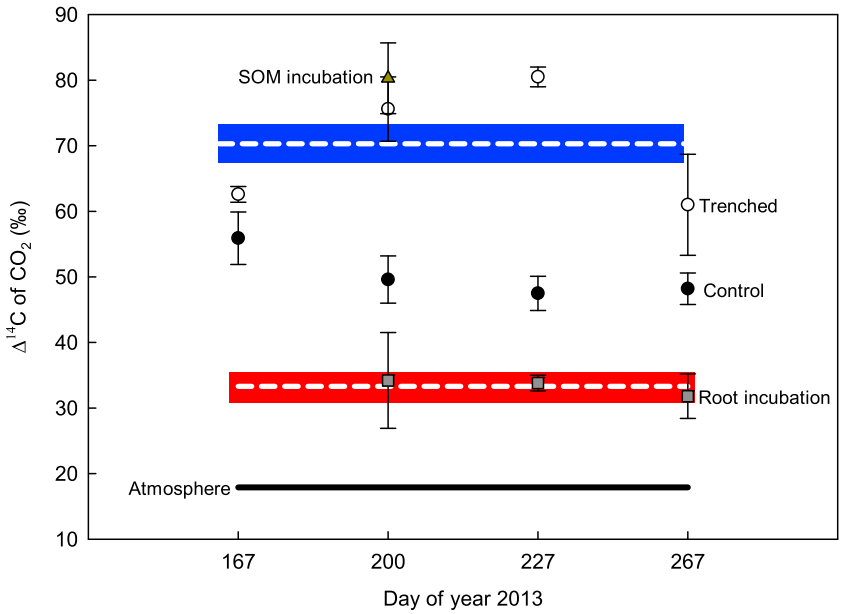

Figure 3. The $\Delta^{14}CO_2$ of samples taken in June through September 2013 at Howland Forest. Control chamber R_s (black circles), trenched chambers (white circles), soil organic matter (SOM) incubations (grey triangle), root incubations (grey squares). Heterotrophic end-member is the mean of SOM incubations and trenched chamber observations shown with white dashed line and blue shading. Autotrophic end-member in the mean of all root incubation observations shown with white dashed line and red shading. Atmospheric canister samples and annual plants shown with black line. Error bars/shading represent ±1 SE.

and 0.56 ± 0.11 (±1 SE, Figure 4), being highest at the beginning of the season on DOY 167. The mean over the four sampling points was 0.58 ± 0.09 from R_a and 0.42 ± 0.09 from R_h. The additional ^{14}C-partitioning scenario using the seasonally varying trenched chamber respiration as the R_h end-member was more variable, and results are shown in Table S1 in the supporting information for comparison.

When the isotopic information was combined with the R_s measurements, seasonal patterns in the partitioned fluxes were driven by large changes in the magnitude of R_s fluxes. R_a more than doubled between DOY 167 and 227. R_h, which varied by only 20% between sampling points, was more stable over the growing season (Figure 5). The mean over the four sampling points was 140.1 ± 33.4 mg C m^{-2} h^{-1} (mean ± 1 SE) from R_a and 97.6 ± 21.6 mg C m^{-2} h^{-1} from R_h.

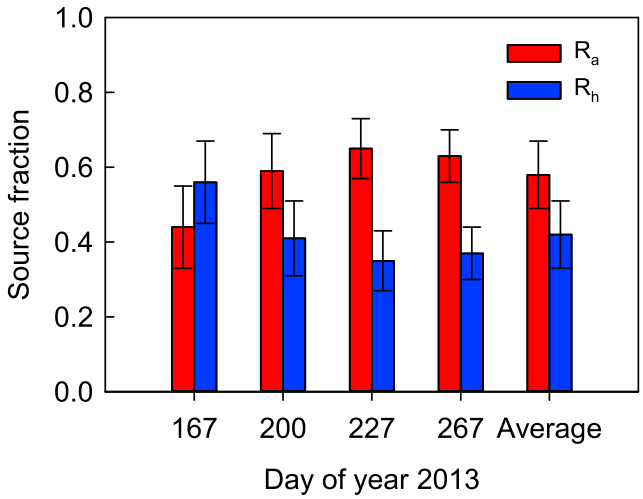

Figure 4. Fractional contribution from autotrophic (R_a, red bars) and heterotrophic (R_h, blue bars) sources to the R_s flux at Howland Forest using the ^{14}C partitioning approach. Error bars represent ±1 SE and include observed variability in the isotopic signatures for the end-members as well as R_s flux following *Phillips and Gregg* [2001].

For comparison, the partitioned fluxes from the trenching experiment are also shown in Figure 5. Day to day variability was large from the trenching study; however, monthly means of the R_h fraction ranged between 0.46 ± 0.11 (DOY 213–243, note that this value is similar in magnitude to the partitioning estimate using the ^{14}C approach) and 0.71 ± 0.14 (DOY 121–151, prior to the ^{14}C measurements). In general, we found greater R_h in the trenching experiment and

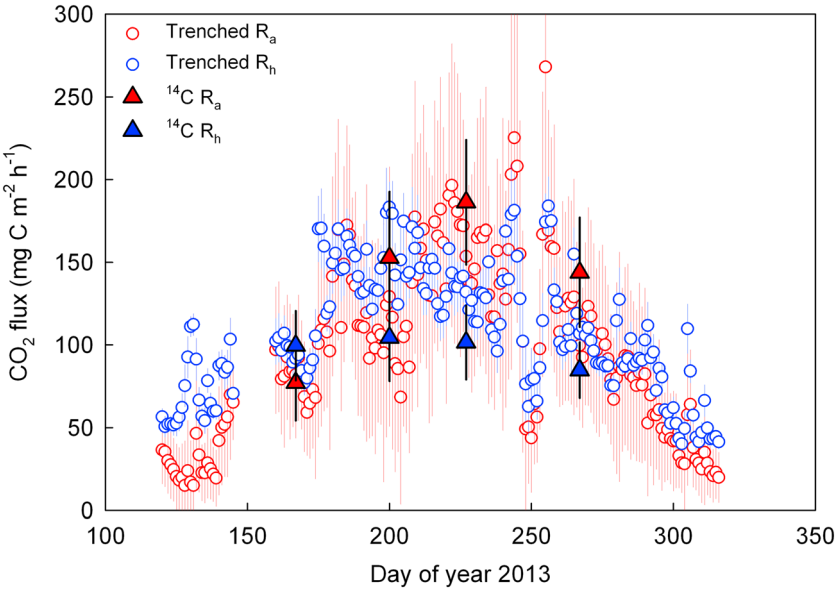

Figure 5. The CO_2 flux from autotrophic (R_a, red) and heterotrophic (R_h, blue) sources as calculated from the trenching (open circles) and the ^{14}C partitioning (closed triangles) approaches. Error bars represent ±1 SE.

greater R_a with the ^{14}C approach. We found large discrepancies between the two approaches only on DOY 200 (Figure 5), where the trenching approach estimated R_h to be greater than R_a by approximately 50%, and the reverse was true for the ^{14}C approach.

3.4. FöBAAR Modeling Current C Cycle—Fluxes

The constrained model predicted substantial interannual variation in C sink strength, with annual net ecosystem exchange (NEE) ranging from about −250 to −350 g C m^{-2} yr^{-1} (Figure 6a). These modeled values are consistent with recent tower-based observations, but higher (~100 g C m^{-2} yr^{-1}) than those observed over the first 5 years of the Howland record. However, in most years there were negligible differences (less than 25 g C m^{-2} yr^{-1}) among model runs in annual NEE with or without the different R_s constraints. The patterns of year-to-year variation in annual NEE were almost identical among model runs. Yet uncertainties—in terms of the width of the 90% confidence interval—on annual NEE were substantially reduced as additional constraints were added and were only half as wide for the R_s-isotope runs (45 g C m^{-2} yr^{-1}) as the R_s-null runs (85 g C m^{-2} yr^{-1}).

Modeled annual gross primary production (GPP) varied by only 15 g C m^{-2} yr^{-1} among runs (and 225 g C m^{-2} yr^{-1} among years) (Figure 6b), while modeled annual ecosystem respiration (R_{eco}) varied by about 25 g C m^{-2} yr^{-1} among runs (and 150 g C m^{-2} yr^{-1} among years) (Figure 6c). However, the patterns of year-to-year variation in annual GPP and R_{eco} were also nearly identical among runs. And again, uncertainties were generally reduced as additional constraints were added.

Not surprisingly, partitioning of R_s to R_a and R_h was only weakly constrained in the R_s-autochamber runs (Figure 6d and 6e), as an increase (decrease) in R_a could be compensated for by a decrease (increase) in R_h to yield the same total R_s. Thus, for the R_s-autochamber runs, the uncertainties on R_a and R_h were as much as three times larger than the uncertainty on total R_s. And, by adding data on partitioning as constraints (R_s-isotope and R_s-trenching runs), the uncertainties on both R_a and R_h were greatly reduced. However, with the best fit model parameters, estimated R_a was about 40% higher for the R_s-isotope run than the R_s-trenching run, while R_h was about 30% higher for the R_s-trenching run than the R_s-isotope run. Importantly, the relatively tight confidence intervals on annual R_a and R_h fluxes were essentially nonoverlapping for the R_s-isotope and R_s-trenching runs (Figure 6d and 6e), indicating that the two partitioning methods yield significantly different estimates of the relative contributions of autotrophic and heterotrophic components to total R_s.

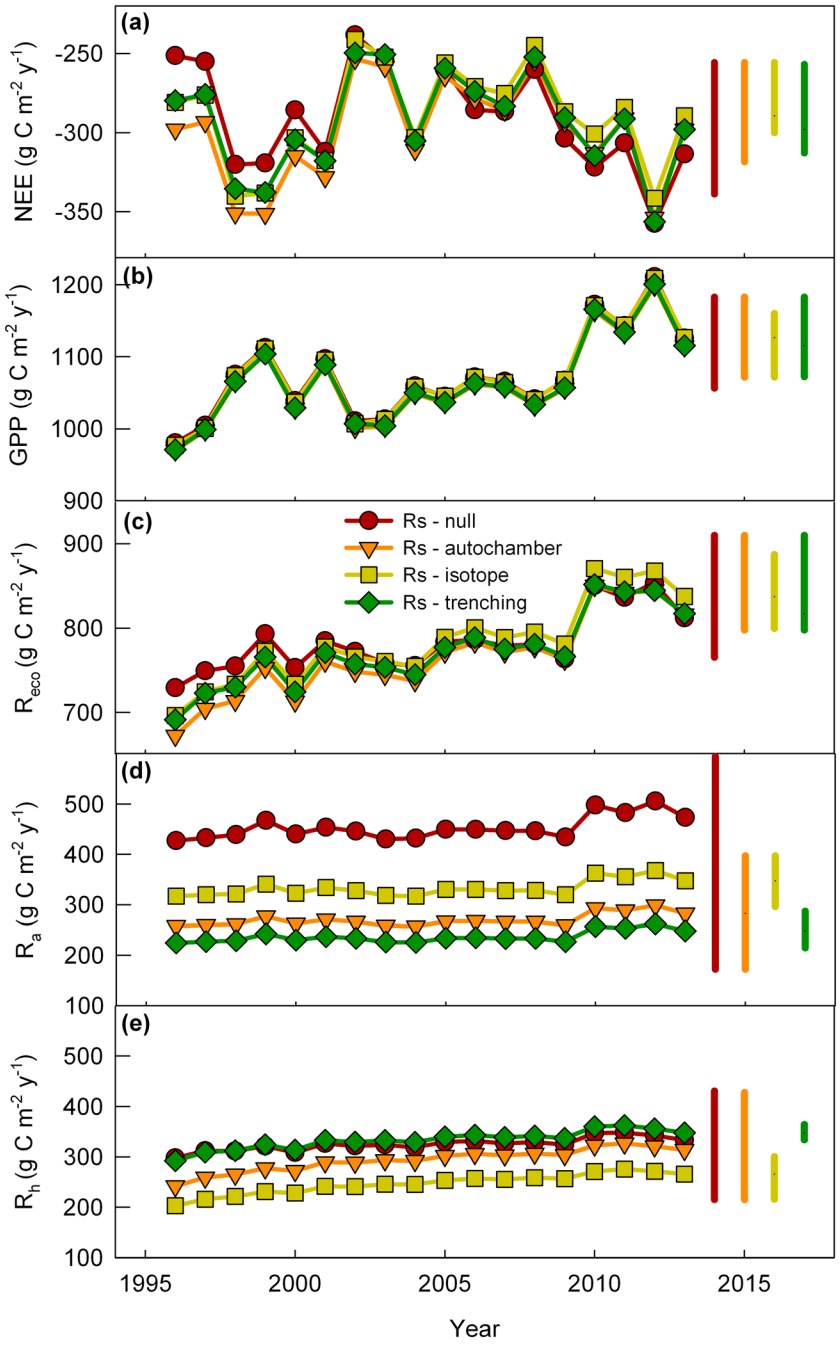

Figure 6. Current model runs: (brown circles) R_s-null run, (orange triangles) R_s-autochamber run, (yellow squares) R_s-isotope run, and (green diamonds) R_s-trenching run with best fit parameters for (a) net ecosystem exchange (NEE), (b) gross primary production (GPP), (c) ecosystem respiration R_{eco}, (d) belowground autotrophic respiration (R_a), and (e) belowground heterotrophic respiration (R_h) from 1996 to 2013. Bars indicate 90% confidence intervals for 2013 only, although uncertainties are similar across all years.

Earlier, we noted that with the ^{14}C approach, we could have used the $\Delta^{14}C$ signature from the trenched plot respiration to obtain a time-varying end-member for R_h. When the calculations were done in this manner, the partitioning was found to be substantially more dynamic. In particular, this approach indicated a very low (0.23 ± 0.14) R_a fraction in June and a very high (0.70 ± 0.06) R_a fraction in August. FöBAAR was unable to reproduce these seasonal patterns. In fact, the fit of the model to these partitioning estimates was about

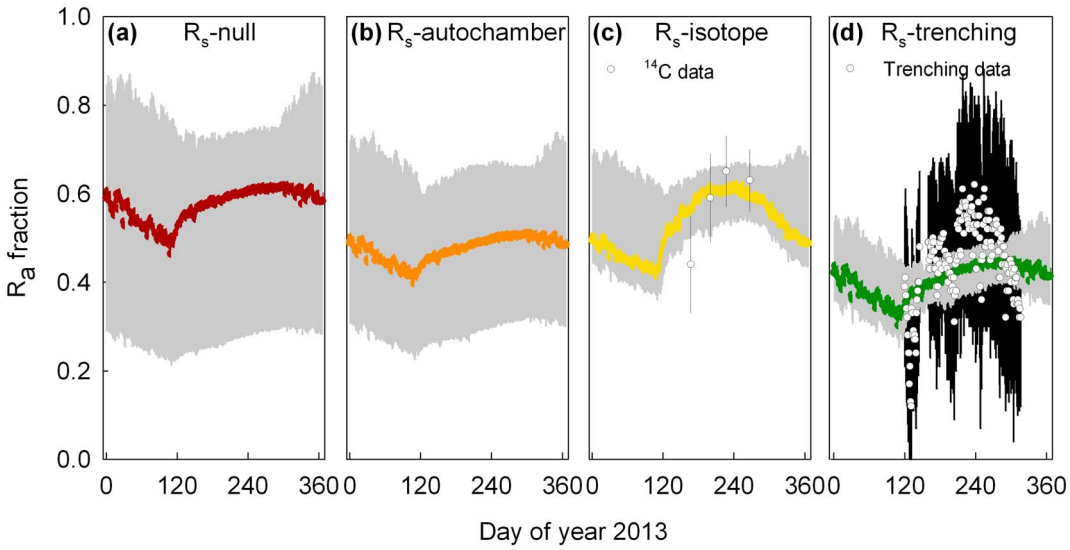

Figure 7. Seasonal variation in the R_a fraction (autotrophic respiration fraction of R_s). Colored symbols indicate model runs: (brown) R_s-null run, (orange) R_s-autochamber run, (yellow) R_s-isotope run, (green) R_s-trenching run with the best fit parameters; shading indicates 90% confidence intervals. The ^{14}C-based partitioning estimates and the trenching-based estimates are shown for reference in white circles on the R_s-isotope and R_s-trenching panels.

twice as poor as for the original R_s-isotope runs. And, because of larger model uncertainties, predictions for both R_a and R_h tended to be not distinguishable from those for either the R_s-isotope or R_s-trenching runs.

3.5. FöBAAR Modeling Current C Cycle—Seasonal Partitioning

Overall, the seasonal trajectory of fluxes and pools was generally similar among model runs, although obvious differences were observed for the seasonal patterns of R_a and R_h and the seasonal amplitude of C_{lit} (see Figure S1).

The relationships among drivers, pool sizes, and fluxes that are implicit in the FöBAAR model structure exerted tight control on the underlying seasonality of the R_a fraction. Indeed, the seasonal variation in R_a fraction tended to be relatively similar, although offset, in the different model runs (Figure 7). Comparing the results for the best fit parameters of each run, the R_a fraction tended to be highest for the R_s-null runs (declining from 0.60 in winter to 0.50 in early spring, then rising to a peak of about 0.65 in early autumn before declining through winter; Figure 7) and lowest for the R_s-trenching runs (similar seasonal pattern, but consistently lower by about 0.20 throughout the year).

The uncertainty in the R_a fraction was extremely large for the R_s-null (about ±0.30, at 90% confidence) and R_s-autochamber (about ±0.20) runs, indicating that without direct constraints on belowground R_a or R_h, it was impossible to separate R_s into its autotrophic and heterotrophic components with any real precision. Substantially narrower uncertainties (about ±0.10) were estimated for both the R_s-isotope and R_s-trenching runs, showing that the observational data were about equally effective in this regard, despite there being only four ^{14}C data points versus several thousand high-frequency trenched plot flux measurements. Notably, however, for R_s-isotope and R_s-trenching the confidence intervals on the R_a fraction were nonoverlapping for much of the year (i.e., from day 120 to day 300).

3.6. FöBAAR Modeling Future C Cycle

Our operating hypothesis was that to the degree that using different observational data constraints would result in the acceptance or rejection of different parameter sets, and hence different partitioning of the R_s into its R_a and R_h components, the associated differences in soil C fluxes would accumulate over time, and be manifest in forward runs as differences in the accretion rates of the litter and soil C pools. To test this hypothesis, we ran the optimized model to 2100, with full uncertainty propagation, using Intergovernmental Panel on Climate Change (IPCC) climate projections.

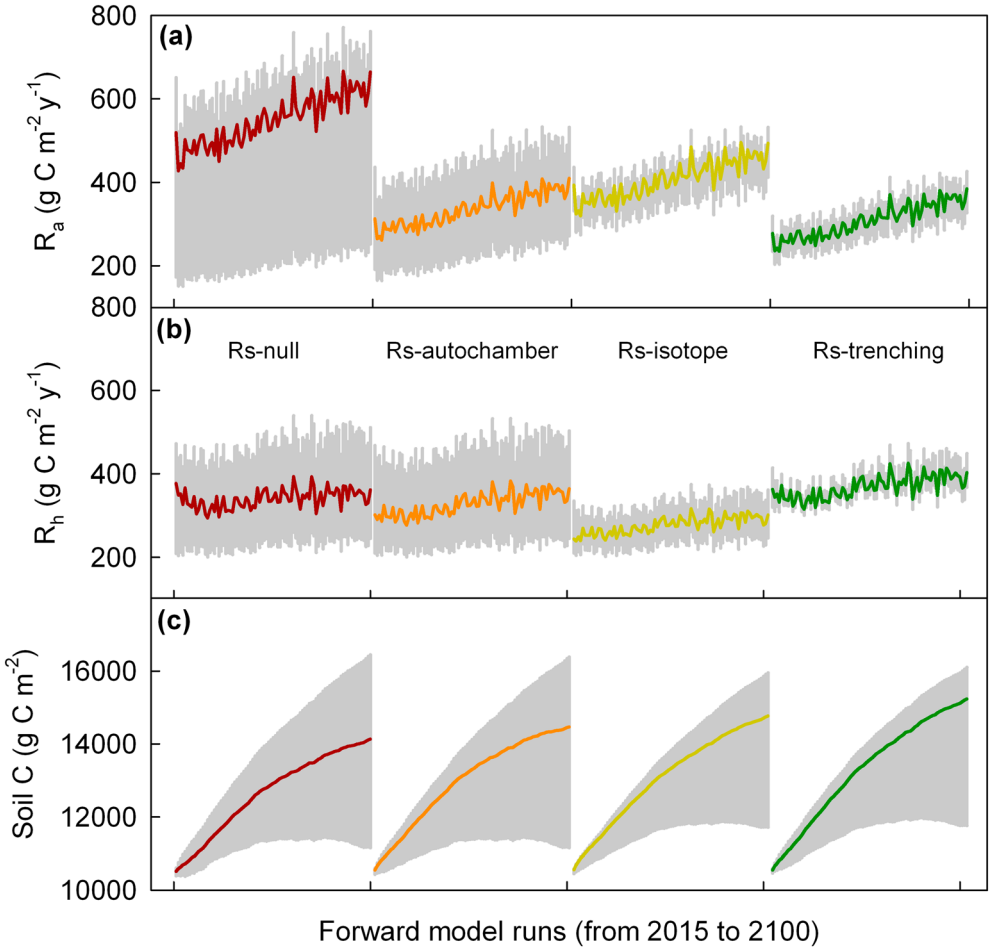

Figure 8. Forward model runs: (brown) R_s-null run, (orange) R_s-autochamber run, (yellow) R_s-isotope run, and (green) R_s-trenching run with the best fit parameters; shading indicates 90% confidence intervals. (a) R_a, autotrophic respiration (b) R_h, heterotrophic respiration, and (c) total soil C. Each "block" is an 85 year run, from 2015 to 2100, conducted using IPCC climate projections.

Overall, our hypothesis was not supported by the results of the forward model runs. In general, although the best fit parameters for each of the four runs generated somewhat different predictions, the confidence intervals for the R_s-isotope and R_s-trenching runs tended to be extremely similar for both ecosystem state variables and for fluxes. There was, for example, an average overlap of almost 80% in the confidence intervals on each of the major C pools at the end of the forward run, and a similar degree of overlap for annual NEE, annual GPP, and annual R_{eco}. The exception to this was that soil C fluxes tended to be quite different between the R_s-isotope and R_s-trenching runs; there was, for example, very little (<10%) overlap in the confidence intervals on annual R_a (higher in R_s-isotope than R_s-trenching), and no overlap in the confidence intervals on annual R_h (lower in R_s-isotope than R_s-trenching), by 2100 (Figures 8a and 8b). However, the temporal changes in the total soil C pool (as well as each of the individual soil C pools) were nevertheless extremely similar among all four model runs, and the confidence intervals were only marginally narrower for the R_s-isotope and R_s-trenching runs than the R_s-null and R_s-autochamber runs (Figure 8c).

4. Discussion

4.1. Trenching and ^{14}C Approaches to R_s Partitioning

Our experimental design of ^{14}C measurements nested within a trenching manipulation with automated R_s measurements allowed for a unique comparison of partitioning approaches. The trenching manipulation enabled us to look at the day-to-day patterns of R_a and R_h. It also allowed us to estimate the cumulative flux

of C respired from each source over the course of the season. Neither of these was possible with the ^{14}C approach, which makes point-in-time measurements that are like snapshots and that require some assumptions to scale the partitioning in time. However, the trenching was also very destructive to the ecosystem, and fluxes from the trenched chambers may have initial artifacts from decomposing roots, and over time, changes in soil moisture and altered fresh C inputs [*Hanson et al.*, 2000]. By comparison, the ^{14}C approach has the advantage that the ecosystem is minimally disturbed, and measurements can be done repeatedly over time without impacting the soil and vegetation where the measurement is taken. Both approaches require significant labor, but sampling for ^{14}C requires also specific expertise, and this approach is more expensive because of the cost of AMS measurements.

We found generally greater R_h in the trenching experiment and greater R_a with the ^{14}C approach. A similar result was found by *Phillips et al.* [2013], who also compared these two methods. Over the measurement period, our trenching experiment indicated that R_h contributed 53 ± 11% of the R_s flux, while the ^{14}C approach indicated that R_h contributed 42 ± 9% of the R_s flux. These values are in agreement with the range of estimates for other temperate and boreal forests [*Bond-Lamberty et al.,* 2004; *Subke et al.,* 2006]. For the individual ^{14}C sampling dates, the two approaches were not always consistent (within the uncertainties). In particular, there are large discrepancies on DOY 200, where the trenching experiment attributed most of the flux to heterotrophic sources and the ^{14}C approach attributed most of the flux to autotrophic sources (Figure 5). Discrepancies between the approaches could be due to aggregate artifacts from the two methodologies. Initially, the trenching treatment increases dead root biomass within the chambers, which can provide substrate for enhanced decomposition for a period of time [*Ewel et al.,* 1987; *Hanson et al.*, 2000]. We estimate this could elevate the R_h fraction six percentage points or more, based on a parallel study using root litter bags at Harvard Forest, Massachusetts, USA (K. Savage, personal communication 2015). Additionally, the ^{14}C approach only distinguishes between young and older C being respired, not specifically R_a and R_h, and therefore, some of the faster cycling (i.e., younger) SOM may be grouped with the autotrophic component (generally younger C) if the heterotrophic end-member (on average older C) is not representative of the source signature. This may be the case if microbial C source is fundamentally different between the ^{14}C method and trenched method as proposed by *Phillips et al.* [2013].

With both approaches, we saw a general seasonal pattern in the fractional partitioning, although it was somewhat offset in time. The R_h fraction was generally higher in the early spring and late fall, and the R_a fraction was consistently higher in the midsummer, when the trees were most active, temperatures were warmest, and when the soil moisture was lowest (perhaps inhibiting surface microbial decomposition) [*Savage and Davidson*, 2001]. The difference in the seasonal estimates of R_a and R_h between the two approaches may simply be due to the different time periods over which they were sampled. The trenching approach extended further into early spring and late summer and captured greater R_h contributions during those time periods. The ^{14}C measurements tended to be centered around midsummer, where we observed greater R_a contributions. However, differences in partitioning estimates between the two approaches were notably persistent when the data were used with the model as constraints.

4.2. Implications for Modeling

In model-data fusion, the addition of observational data constraints that contribute new information to the optimization has been shown to substantially reduce model uncertainties [*Richardson et al.,* 2010; *Ricciuto et al.,* 2011; *Keenan et al.,* 2013b; *Du et al.,* 2015]. Here our goal was to test whether the addition of R_s and partitioning data contributed to reduced uncertainties on C fluxes and pools in the ecosystem model FöBAAR.

It has long been acknowledged that a model is only as good as the data on which it is based. In a model-data fusion context, this aphorism has two essential elements: (1) data uncertainties are a measure of confidence in the data, and data with smaller uncertainties effectively received greater weight in the optimization [*Raupach et al.,* 2005]. Thus, data with large uncertainties—or data in which we have low confidence—will not contribute substantially to better constraining model parameters; (2) biased data will cause bias in estimated model parameters or states [*Williams et al.,* 2009]. This applies not only to our partitioning estimates but also to the overall ecosystem C balance: a critical but generally ignored source of bias in C-cycle model-data fusion analyses is in the eddy covariance flux data themselves. We do not believe that this is a major source of bias in our model, as Howland has flat, homogeneous terrain and is nearly ideal as a flux site

[*Hollinger et al*., 1999, 2004]. On the other hand, we have observed a not-fully-explained increase in net ecosystem C uptake over the course of our measurements [*Keenan et al.,* 2013a; *Holmes*, 2014] and with our century-long model run, even small biases in NEE (e.g., 10 g C m^{-2} yr^{-1}) have the potential to add up to a substantial amount (e.g., 10 g C m^{-2} yr^{-1} × 100 yr = 1000 g C m^{-2} yr^{-1}) of additional C stored in the ecosystem.

Additionally, multiconstraint optimization poses a challenge because there is not an unambiguous, uniquely optimal parameter set. That is, the constrained model can never fit the data perfectly, and improving fit to one data stream typically must come at the cost of worse fit to one or more other data streams [*Gupta et al.,* 1999]. So compared to the model fit achieved in the R_s-autochamber runs, the R_s-isotope and R_s-trenching runs tended to do a bit (but not much) worse against NEE, R_s, evapotranspiration, and woody biomass increment data, in order to get a better fit to the ^{14}C data and trenched plot fluxes, respectively (see Table S2). A key implication of this is that unless *all* fluxes and pools are directly constrained with data, the model is likely to be over-fit to those fluxes and pools that have been constrained. And, by extension, caution should be exercised in the interpretation of those fluxes and pools that have not been directly constrained, as these may be (and most likely are) completely unreliable [*Dietze et al.,* 2013]. Full propagation of uncertainties is therefore critical because this method can be used to identify and rank these "known unknowns," which can be selectively targeted for additional measurement effort [*Richardson et al.,* 2010].

In all model runs, temporal changes in simulated soil C pools were large but also highly uncertain. We note that while the aboveground biomass sink is constrained by data, the soil C sink is not (and, as discussed below, the R_s partitioning data were of little help in this regard). Our tower measurements indicate annual (gap-filled) NEE over the 1996–2013 period is approximately 215 ± 60 ± 60 g C m^{-2} yr^{-1} (mean ± SD across years ± average uncertainty for an individual year), while measured annual woody biomass increment (ΔCw) is about 160 ± 11 ± 16 g C m^{-2} yr^{-1}. Because the model enforces mass balance, then (assuming the foliage biomass pool is approximately in steady state) this leaves a residual of about 55 g C m^{-2} yr^{-1} which is inevitably allocated to those C pools which are not constrained, principally SOM. And any possible model overestimate of NEE would likely result in further overestimation of this poorly constrained soil C sink. Indeed, for the current climate runs, the modeled NEE (−290 ± 75 g C m^{-2} yr^{-1}, mean ± 1 SD across years) was about 75 g C m^{-2} yr^{-1} larger, or more negative, than the gap-filled NEE, with the ultimate fate of most of this "extra" C being belowground, as SOM. We acknowledge that the resulting model estimates of changes in soil C are higher than generally accepted values for temperate forests [*Schlesinger*, 1990; *Richter et al.,* 1999; *Paul et al.,* 2002; *Lilienfein et al.,* 2003; *Jandl et al.,* 2007; *Yang et al.,* 2011], although repeat studies have general found greater accumulation than chronosequence studies [*Gleixner et al.,* 2009]. We also note that the uncertainties are so large on our forward runs that they include not only very high but also very low rates of SOM accretion and are thus not inconsistent with these other studies.

A surprising result to emerge from our analysis was that differences among model runs in the partitioning of R_s flux to R_a and R_h components did not translate into differences in the accretion rates of soil C pools during the forward run (and, sensitivity analyses shown in Figures S3a–S3e confirm that this is a more general result). This indicates that while the partitioning data allow us to distinguish the contributions of R_a and R_h to total soil C efflux, they do not reduce uncertainties on long-term changes in SOM, suggesting that the partitioning information provides redundant information on fast-turnover pools but not the slow-turnover pools that determine decadal-to-century SOM trajectories. And an interpretation of this is that the model parameterization must have shifted in different runs to reflect corresponding shifts in C allocation, and/or decomposition rates. Confidence intervals on the base rates, temperature sensitivities, and decomposition:respiration ratios did not vary substantially R_s-isotope and R_s-trenching runs (Figure S2), but overall the main allocation shift between the R_s-isotope and the R_s-trenching run under future climate was a decrease in R_a (410 g C m^{-2} yr^{-1} versus 310 g C m^{-2} yr^{-1}, respectively). This was accompanied by an increase in root litter production (160 g C m^{-2} yr^{-1} in the R_s-isotope run, versus 250 g C m^{-2} yr^{-1} in the R_s-trenching run), which then enabled correspondingly higher rates of R_h (280 g C m^{-2} yr^{-1} in the R_s-isotope run, versus 370 g C m^{-2} yr^{-1} in the R_s-trenching run), resulting in only a negligible difference in the mean annual rate of SOM accretion by 2100 (50 g C m^{-2} yr^{-1} in the R_s-isotope run, versus 55 g C m^{-2} yr^{-1} in the R_s-trenching run; in both cases the confidence intervals were large, ranging from 15 to 65 g C m^{-2} yr^{-1}). In essence, increased allocation of C to fine root litter production in the R_s-trenching run increases C inputs to the fast soil C pool. However, the fate of most of the C in the fast pool is to be respired back to the atmosphere.

Thus, very little of this increased C input is transferred to more stabilized SOM pools with longer residence times (e.g., slow and passive pools), and therefore, differences in SOM accumulation between R_s-trenching and R_s-isotope runs were negligible despite large differences in R_h fluxes between the two runs.

On the basis of the above, we hypothesized that adding new data (tighter constraints) on either total C input to the system or long-term changes in SOM pool sizes would presumably contribute to reducing uncertainties and potential biases in modeled rates of SOM accretion. To test this, we conducted additional model runs using hypothetical data constraints. We found that either by forcing lower rates of annual NEE (i.e., so that the difference between annual NEE and annual ΔCw was approximately zero), or by constraining the annual change in total SOM to be $< 15 \pm 5$ g C m^{-2} yr^{-1}, annual rates of SOM accretion in the current climate runs could be brought in line with the published values described above. But while rates of future SOM accretion were also reduced compared to any of the runs illustrated in Figure 8, the uncertainties on these rates of accretion generally remained large (see Figures S3f–S3i), presumably because of unconstrained allocation parameters and/or poorly constrained turnover times for the different SOM pools.

Finally, we note that the results of any model-data fusion exercise are implicitly dependent on the underlying model structure. For example, the use of a model with more explicit representation of microbial processes, priming effects, nutrient limitation, or SOM stabilization processes might lead to different conclusions about the fate of C inputs to the soil, especially when model runs are conducted on timescales of decades-to-centuries with changing climate and CO_2 concentrations [e.g., *Friedlingstein et al.,* 2006; *Wieder et al.,* 2015; *Luo et al.,* 2016].

5. Conclusions

In conclusion, we found that the two partitioning approaches, root trenching, and the ^{14}C mass balance, quantified autotrophic and heterotrophic sources differently, yet provided valuable information for modeling of the C cycle under current and future climatic conditions. Our results show that incorporating field-based data constraints of the autotrophic and heterotrophic partitioning considerably reduces model uncertainties of soil C fluxes, but not soil C pools. However, we also show that the modeling results are sensitive to the partitioning method used. And unexpectedly, the impact of these partitioning constraints on the modeled soil C pool sizes may be small when run forward with future climate and CO_2 scenarios without having additional constraints on other C pools and fluxes, such as plant C allocation and SOM turnover.

Acknowledgments

In line with the AGU publications data policy, the ^{14}C data used in this paper can be accessed in results section 12, and the flux and biometric data for Howland Forest used for modeling is available through the FLUXNET website (http://fluxnet.ornl.gov/site/890), a component of the Oak Ridge National Laboratory DAAC. Funding for this work was provided by the U.S. Department of Energy's Office of Science and the U.S. Forest Service Northern Research Station and by USDA grant 2014-67003-22073 to the Woods Hole Research Center, with subcontracts to Harvard University and the University of Maryland Center for Environmental Science. We thank Robert Evans, John Lee, Miriam Stevens, and Donald Aubrecht for assistance in the field and lab. Katherine Heckman and Timothy Veverica provided assistance with ^{14}C analyses, which was supported by the Radiocarbon Collaborative and jointly sponsored by the USDA Forest Service, Lawrence Livermore National Laboratory, and Michigan Technological University.

References

Ahrens, B., M. Reichstein, W. Borken, J. Muhr, S. E. Trumbore, and T. Wutzler (2014), Bayesian calibration of a soil organic carbon model using δ^{14}C measurements of soil organic carbon and heterotrophic respiration as joint constraints, *Biogeosciences*, *11*(8), 2147–2168, doi:10.5194/bg-11-2147-2014.

Bond-Lamberty, B., C. K. Wang, and S. T. Gower (2004), Contribution of root respiration to soil surface CO_2 flux in a boreal black spruce chronosequence, *Tree Physiol.*, *24*(12), 1387–1395.

Boone, R. D., K. J. Nadelhoffer, J. D. Canary, and J. P. Kaye (1998), Roots exert a strong influence on the temperature sensitivity of soil respiration, *Nature*, *396*, 570–572.

Brekke, L., B. L. Thrasher, E. P. Maurer, and T. Pruitt (2013), Downscaled CMIP3 and CMIP5 climate projections, *U.S. Dep. Inter. Bur. Reclamation, Tech. Serv. Cent*.

Carbone, M. S., G. C. Winston, and S. E. Trumbore (2008), Soil respiration in perennial grass and shrub ecosystems: Linking environmental controls with plant and microbial sources on seasonal and diel timescales, *J. Geophys. Res.*, *113*, G02022, doi:10.1029/2007JG000611.

Carbone, M. S., C. J. Still, A. R. Ambrose, T. E. Dawson, A. P. Williams, C. M. Boot, S. M. Schaeffer, and J. P. Schimel (2011), Seasonal and episodic moisture controls on plant and microbial contributions to soil respiration, *Oecologia*, *167*, 265–278, doi:10.1007/s00442-011-1975-3.

Davidson, E. A., and N. M. Holbrook (2009), Is temporal variation of soil respiration linked to the phenology of photosynthesis? in *Phenology of Ecosystem Processes: Applications in Global Change Research*, pp. 187–199, New York.

Davidson, E. A., A. D. Richardson, K. E. Savage, and D. Y. Hollinger (2006), A distinct seasonal pattern of the ratio of soil respiration to total ecosystem respiration in a spruce-dominated forest, *Global Change Biol.*, *12*(2), 230–239, doi:10.1111/j.1365-2486.2005.01062.x.

Davis, J. C., et al. (1990), LLNL/UC AMS facility and research program, *Nucl. Instrum. Methods Phys. Res. Sect. B Beam Interact. Mater. Atoms*, *52*(3–4), 269–272, doi:10.1016/0168-583X(90)90419-U.

Dietze, M. C., D. S. Lebauer, and R. Kooper (2013), On improving the communication between models and data, *Plant Cell Environ.*, *36*(9), 1575–1585, doi:10.1111/pce.12043.

Du, Z., Y. Nie, Y. He, G. Yu, H. Wang, and X. Zhou (2015), Complementarity of flux- and biometric-based data to constrain parameters in a terrestrial carbon model, *Tellus B*, *67*, doi:10.3402/tellusb.v67.24102.

Ewel, K., W. P. Cropper, and H. Gholz (1987), Soil CO_2 evolution in Florida slash pine plantations. II Importance of root respiration, *Can. J. For. Res.*, *17*, 330–333, doi:10.1139/cjfr-17-4-330.

Fernandez, I. J., L. E. Rustad, and G. B. Lawrence (1993), Estimating total soil mass, nutrient content, and trace metals in soils under a low elevation spruce-fir forest, *Can. J. Soil Sci.*, *73*(3), 317–328, doi:10.4141/cjss93-034.

Fox, A., et al. (2009), The REFLEX project: Comparing different algorithms and implementations for the inversion of a terrestrial ecosystem model against eddy covariance data, *Agric. For. Meteorol.*, *149*, 1597–1615, doi:10.1016/j.agrformet.2009.05.002.

Friedlingstein, P., et al. (2006), Climate–carbon cycle feedback analysis: Results from the C^4MIP model intercomparison, *J. Clim.*, *19*, 3337–3353, doi:10.1175/JCLI3800.1.

Gaudinski, J., S. Trumbore, and E. Davidson (2000), Soil carbon cycling in a temperate forest: Radiocarbon-based estimates of residence times, sequestration rates and partitioning of fluxes, *Biogeochemistry*, *51*, 33–69.

Gleixner, G., C. Tefs, A. Jordan, M. Hammer, C. Wirth, A. Nueske, A. Telz, U. E. Schmidt, and S. Glatzel (2009), *Soil Carbon in Old-Growth Forests*, *Old-Growth*, edited by C. Wirth, G. Gleixner, and M. Heimann, Springer, Heidelberg.

Gu, L., P. J. Hanson, W. Mac Post, and Q. Liu (2008), A novel approach for identifying the true temperature sensitivity from soil respiration measurements, *Global Biogeochem. Cycles*, *22*, GB4009, doi:10.1029/2007GB003164.

Gupta, H. V., L. A. Bastidas, S. Sorooshian, W. J. Shuttleworth, and Z. L. Yang (1999), Parameter estimation of a land surface scheme using multicriteria methods, *J. Geophys. Res.*, *104*(D16), 19,491–19,503, doi:10.1029/1999JD900154.

Hanson, P. J., N. T. Edwards, C. T. Garten, and J. A. Andrews (2000), Separating root and soil microbial contributions to soil respiration: A review of methods and observations, *Biogeochemistry*, *48*(1), 115–146.

Heinemeyer, A., I. P. Hartley, S. P. Evans, J. A. Carreira De La Fuente, and P. Ineson (2007), Forest soil CO_2 flux: Uncovering the contribution and environmental responses of ectomycorrhizas, *Glob. Chang. Biol.*, *13*(8), 1786–1797, doi:10.1111/j.1365-2486.2007.01383.x.

Hollinger, D. Y., S. M. Goltz, E.a Davidson, J. T. Lee, K. Tu, and H. T. Valentine (1999), Seasonal patterns and environmental control of carbon dioxide and water vapour exchange in an ecotonal boreal forest, *Global Change Biol.*, *5*(8), 891–902, doi:10.1046/j.1365-2486.1999.00281.x.

Hollinger, D. Y., et al. (2004), Spatial and temporal variability in forest-atmosphere CO_2 exchange, *Global Change Biol.*, *10*(10), 1689–1706, doi:10.1111/j.1365-2486.2004.00847.x.

Holmes, C. D. (2014), Air pollution and forest water use, *Nature*, *507*(7491), E1–E2, doi:10.1038/nature13113.

Jandl, R., M. Lindner, L. Vesterdal, B. Bauwens, R. Baritz, F. Hagedorn, D. W. Johnson, K. Minkkinen, and K. A. Byrne (2007), How strongly can forest management influence soil carbon sequestration?, *Geoderma*, *137*(3–4), 253–268, doi:10.1016/j.geoderma.2006.09.003.

Keenan, T. F., M. S. Carbone, M. Reichstein, and A. D. Richardson (2011), The model-data fusion pitfall: Assuming certainty in an uncertain world, *Oecologia*, *167*, 587–597, doi:10.1007/s00442-011-2106-x.

Keenan, T. F., E. Davidson, A. M. Moffat, W. Munger, and A. D. Richardson (2012), Using model-data fusion to interpret past trends, and quantify uncertainties in future projections, of terrestrial ecosystem carbon cycling, *Global Change Biol.*, *18*(8), 2555–2569, doi:10.1111/j.1365-2486.2012.02684.x.

Keenan, T. F., D. Y. Hollinger, G. Bohrer, D. Dragoni, J. W. Munger, and H. P. Schmid (2013a), Increase in forest water-use efficiency as atmospheric carbon dioxide concentrations rise, *Nature*, *499*, 324–327, doi:10.1017/CBO9781107415324.004.

Keenan, T. F., E. A. Davidson, J. W. Munger, and A. D. Richardson (2013b), Rate my data: Quantifying the value of ecological data for the development of models of the terrestrial carbon cycle, *Ecol. Appl.*, *23*, 273–286, doi:10.1890/12-0747.1.

Kuzyakov, Y. (2006), Sources of CO_2 efflux from soil and review of partitioning methods, *Soil Biol. Biochem.*, *38*, 425–448, doi:10.1016/j.soilbio.2005.08.020.

Kuzyakov, Y., and O. Gavrichkova (2010), REVIEW: Time lag between photosynthesis and carbon dioxide efflux from soil: A review of mechanisms and controls, *Global Change Biol.*, *16*(12), 3386–3406, doi:10.1111/j.1365-2486.2010.02179.x.

Lilienfein, J., R. G. Qualls, S. M. Uselman, and S. D. Bridgham (2003), Soil formation and organic matter accretion in a young andesitic chronosequence at Mt. Shasta, California, *Geoderma*, *116*(3–4), 249–264, doi:10.1016/S0016-7061(03)00086-7.

Luo, Y., et al. (2016), Toward more realistic projections of soil carbon dynamics by Earth system models, *Global Biogeochem. Cycles*, *30*, 40–56, doi:10.1002/2015GB005239.

Moyano, F. E., et al. (2012), The moisture response of soil heterotrophic respiration: Interaction with soil properties, *Biogeosciences*, *9*(3), 1173–1182, doi:10.5194/bg-9-1173-2012.

Ogle, K., and E. Pendall (2015), Isotope partitioning of soil respiration: A Bayesian solution to accommodate multiple sources of variability, *J. Geophys. Res. Biogeosci.*, *120*, 221–236, doi:10.1002/2014JG002794.

Paul, K. I., P. J. Polglase, J. G. Nyakuengama, and P. K. Khanna (2002), Change in soil carbon following afforestation, *For. Ecol. Manage.*, *168*(1–3), 241–257, doi:10.1016/S0378-1127(01)00740-X.

Phillips, C. L., K. J. McFarlane, D. Risk, and A. R. Desai (2013), Biological and physical influences on soil $^{14}CO_2$ seasonal dynamics in a temperate hardwood forest, *Biogeosciences*, *10*(12), 7999–8012, doi:10.5194/bg-10-7999-2013.

Phillips, D. L., and J. W. Gregg (2001), Uncertainty in source partitioning using stable isotopes, *Oecologia*, *127*(February), 171–179, doi:10.1007/s004420000578.

Pregitzer, K. S., J. A. King, A. J. Burton, and S. E. Brown (2000), Responses of tree fine roots to temperature, *New Phytol.*, *147*(1), 105–115.

Press, W., B. Flannery, S. Teukolsky, and W. Vetterling (1993), *Numerical Recipes in Fortran 77: The Art of Scientific Computing*, Cambridge Univ. Press, Cambridge.

Raich, J. W., and W. H. Schlesinger (1992), The global carbon dioxide flux in soil respiration and its relationship to vegetation and climate, *Tellus B*, *44*(2), 81–99, doi:10.1034/j.1600-0889.1992.t01-1-00001.x.

Raupach, M. R., P. J. Rayner, D. J. Barrett, R. S. Defries, M. Heimann, D. S. Ojima, S. Quegan, and C. C. Schmullius (2005), Model-data synthesis in terrestrial carbon observation: Methods, data requirements and data uncertainty specifications, *Global Change Biol.*, *11*(3), 378–397, doi:10.1111/j.1365-2486.2005.00917.x.

Ricciuto, D. M., A. W. King, D. Dragoni, and W. M. Post (2011), Parameter and prediction uncertainty in an optimized terrestrial carbon cycle model: Effects of constraining variables and data record length, *J. Geophys. Res.*, *116*, G01033, doi:10.1029/2010JG001400.

Richardson, A. D., et al. (2010), Estimating parameters of a forest ecosystem C model with measurements of stocks and fluxes as joint constraints, *Oecologia*, *164*, 25–40, doi:10.1007/s00442-010-1628-y.

Richter, D. D., D. Markewitz, S. E. Trumbore, and C. G. Wells (1999), Rapid accumulation and turnover of soil carbon in a re-establishing forest, *Nature*, *400*(6739), 56–58, doi:10.1038/21867.

Savage, K. E., and E. A. Davidson (2001), Interannual variation of soil respiration in two New England forests, *Global Biogeochem. Cycles*, *15*(2), 337–350, doi:10.1029/1999GB001248.

Savage, K. E., and E. A. Davidson (2003), A comparison of manual and automated systems for soil CO_2 flux measurements: Trade-offs between spatial and temporal resolution, *J. Exp. Bot.*, *54*(384), 891–899, doi:10.1093/jxb/erg121.

Savage, K., E. A. Davidson, and A. D. Richardson (2008), A conceptual and practical approach to data quality and analysis procedures for high-frequency soil respiration measurements, *Funct. Ecol.*, *22*(6), 1000–1007, doi:10.1111/j.1365-2435.2008.01414.x.

Savage, K., E. A. Davidson, A. D. Richardson, and D. Y. Hollinger (2009), Three scales of temporal resolution from automated soil respiration measurements, *Agric. For. Meteorol.*, *149*(2009), 2012–2021, doi:10.1016/j.agrformet.2009.07.008.

Savage, K., E. A. Davidson, and J. Tang (2013), Diel patterns of autotrophic and heterotrophic respiration among phenological stages, *Global Change Biol.*, *19*(4), 1151–1159, doi:10.1111/gcb.12108.

Schlesinger, W. H. (1990), Evidence from chronosequence studies for a low carbon-storage potential of soils, *Nature*, *348*(6298), 232–234, doi:10.1038/348232a0.

Schulze, E. D., et al. (2010), The European carbon balance. Part 4: Integration of carbon and other trace-gas fluxes, *Global Change Biol.*, *16*(5), 1451–1469, doi:10.1111/j.1365-2486.2010.02215.x.

Schuur, E. A. G., and S. E. Trumbore (2006), Partitioning sources of soil respiration in boreal black spruce forest using radiocarbon, *Global Change Biol.*, *12*(2), 165–176, doi:10.1111/j.1365-2486.2005.01066.x.

Stuiver, M., and H. A. Polach (1977), Reporting of C-14 data—Discussion, *Radiocarbon*, *19*(3), 355–363.

Subke, J. A., I. Inglima, and M. F. Cotrufo (2006), Trends and methodological impacts in soil CO2 efflux partitioning: A metaanalytical review, *Global Change Biol.*, *12*(6), 921–943, doi:10.1111/j.1365-2486.2006.01117.x.

Trudinger, C. M., et al. (2007), OptIC project: An intercomparison of optimization techniques for parameter estimation in terrestrial biogeochemical models, *J. Geophys. Res.*, *112*, G02027, doi:10.1029/2006JG000367.

Trumbore, S. (2006), Carbon respired by terrestrial ecosystems—Recent progress and challenges, *Global Change Biol.*, *2*, 141–153, doi:10.1111/j.1365-2486.2005.01067.x.

Vogel, J. S., J. R. Southon, and D. E. Nelson (1987), Catalyst and binder effects in the use of filamentous graphite for AMS, *Nucl. Instrum. Methods Phys. Res. Sect. B Beam Interact. Mater. Atoms*, *29*, 50–56, doi:10.1016/0168-583X(87)90202-3.

Wieder, W. R., et al. (2015), Explicitly representing soil microbial processes in Earth system models, *Global Biogeochem. Cycles*, *29*, 1782–1800, doi:10.1002/2015GB005188.

Williams, M., et al. (2009), Improving land surface models with FLUXNET data, *Biogeosci. Discuss.*, *6*(2), 2785–2835, doi:10.5194/bgd-6-2785-2009.

Yang, Y., Y. Luo, and A. C. Finzi (2011), Carbon and nitrogen dynamics during forest stand development: A global synthesis, *New Phytol.*, *190*(4), 977–989, doi:10.1111/j.1469-8137.2011.03645.x.

Zobitz, J. M., D. J. P. Moore, W. J. Sacks, R. K. Monson, D. R. Bowling, and D. S. Schimel (2008), Integration of process-based soil respiration models with whole-ecosystem CO_2 measurements, *Ecosystems*, *11*(2), 250–269, doi:10.1007/s10021-007-9120-1.